Modulations in the CuO Chain Layer of $YBa_2Cu_3O_{7-\delta}$: Charge Density Waves?

H. L. Edwards, A. L. Barr, J. T. Markert, and A. L. de Lozanne*
Department of Physics, The University of Texas, Austin, Texas 78712-1081
(Received 9 May 1994)

We have performed reversed-bias scanning tunneling microscopy at 20 K on the CuO chain layer of cold-cleaved single crystals of $YBa_2Cu_3O_{7-\delta}$. We find 1.3-nm corrugations which change sign under bias polarity reversal. This behavior and the 1.3-nm wavelength are in agreement with the hypothesis that the one-dimensional CuO chains undergo a charge density wave transition. This is the first real-space evidence of such a transition in $YBa_2Cu_3O_{7-\delta}$. We also explore the possibility that the corrugations are caused by Friedel oscillations or bipolaron scattering. Several-nm depressions along the CuO chains transform into broad swells and depressions as the bias voltage is increased.

PACS numbers: 74.50.+r, 61.16.Ch, 74.72.Bk

The search for a basic understanding of high-temperature superconductivity (HTSC) has been slowed by the complex chemical and electronic nature of the oxide superconductors. For instance, lattice instabilities have been found to accompany the onset of superconductivity in several HTSC. Pair distribution function analysis (PDF) of neutron-scattering data has found locally correlated ionic displacements for temperatures below the superconducting T_c in $La_{2-x}Sr_xCuO_4$, $Tl_2Ba_2CaCu_2O_8$, $(Ba_{0.6}K_{0.4})BiO_3$, and $Nd_{2-x}Ce_xCuO_{4-y}$. The CuO-chain oxygen ions in $YBa_2Cu_4O_8$ (124) undergo correlated displacements in the **a** (out-of-chain) direction of about 0.01 nm, with the onset of correlations occurring near 150 K; a similar effect is observed in $YBa_2Cu_3O_{7-\delta}$ (123) [1]. Ion channeling and x-ray absorption fine structure (XAFS) have identified correlated ionic displacements with an onset at T_c [2].

In addition to data regarding ionic motion, there is evidence that the electronic structure of the CuO chains in 123 is unusual. Infrared reflectivity [3] data exhibits peaks in the **b**-direction conductivity which can be explained [4] by a charge density wave (CDW) in the CuO chains. Thus, there is a wide array of evidence that the electrons and ions in the one-dimensional CuO chains undergo some sort of collective phenomenon. However, all of these analytical techniques must be regarded as indirect, since they obtain either reciprocal-space or spatially averaged information. From spatially averaged data, it is difficult to separate the contribution of the CuO chains from that of the CuO_2 planes.

In this Letter, we present atomically resolved real-space evidence that the CuO chain electrons do participate in such a collective phenomenon in 123. Using reversed-bias scanning tunneling microscopy (STM) at 20 K, we have identified corrugations in the electron density along the CuO chains which have a periodicity of several lattice constants, and reverse sign under bias reversal. We consider the possibilities that these corrugations are due to a CDW state, Friedel oscillations, or bipolarons.

In previous work [5], we obtained atomic-resolution STM images and reproducible scanning tunneling spectroscopy (STS) ($2\Delta/kT_c = 6-8$) of the cold-cleaved **c**-normal surface of high-quality single crystals of 123. In that work, we found that 123 cleaves between the CuO chain and BaO plane layers. That conclusion has been supported by more recent work [6], and was arrived at independently by photoemission studies on cold-cleaved 123 single crystals [7]. Scanning Auger microscopy [8] indicates that 123 cleaves between the BaO and CuO_2 planes as well as between the BaO and CuO chain layers.

The CuO chain images display several striking features: several-nm *depressions,* 1.3-nm *corrugations,* and *atomic bumps.* Several-nm *depressions* exist along individual chains in the STM images [5,6]; a given depression is confined to a single CuO chain, and there is no long-range order to the placement of these depressions. In addition, the spatial density of the depressions is consistent with the expected density of oxygen vacancies in a good 123 single crystal, $\delta = 0.05$ [6]. Since the only well-known point defects in the CuO chains are oxygen vacancies, we interpret the several-nm depressions as being due to oxygen vacancies.

In all of the CuO-chain STM images, we have observed *corrugations* along the chains which were several lattice constants ($b = 0.4$ nm) in wavelength. These corrugations along the CuO chains are strongest near the depressions and the corrugations along nearby chains are correlated (they tend to align with each other), but they do not exhibit long-range order. This lack of long-range order would hide these corrugations as well as the depressions from detection by diffraction techniques. Recently, we have studied [6] the CuO chain layer with reversed-bias STM imaging, and found the unexpected result that these corrugations change sign (or shift phase by 180°) when the bias polarity is reversed. The behavior of these corrugations is more complex in the depressions [6], probably due to the crystal field perturbation of the oxygen vacancies. Here we concentrate on the reversed-bias behavior of the CuO chains away from depressions.

In addition to the depressions and corrugations, we have obtained a smaller number of STM images in which *atomic bumps* are observed along the CuO chains.

0031-9007/94/73(8)/1154(4)$06.00

These atomic features are separated by b, and appear in addition to the 1.3-nm corrugations, allowing an accurate determination of the wavelength of the corrugations to be made. We obtained [6] 1.3 ± 0.1 nm, which is approximately $3b$.

Figure 1 shows reversed-bias images of the CuO chain layer, with positive sample bias in 1(a) and negative sample bias in 1(b). Figure 1(c) is the average, and 1(d) the difference (divided by 2), of 1(a) and 1(b). These data show the same reversed-bias behavior as our earlier work [6]. In Fig. 1(e) we show a cross section of 1(a)–1(d) along a CuO chain, away from a depression, which shows four 1.3-nm corrugations and their behavior under bias reversal.

Figure 2 shows a reversed-bias image [2(a) and 2(b)] during which the tip underwent a sudden change, resulting in atomic resolution along the CuO chains for the bottom 2/3 of the image. Figure 2(c) is the difference of 2(a) and 2(b), and shows the 1.3-nm corrugations more strongly than either 2(a) or 2(b), whereas the depressions, common to 2(a) and 2(b), do not appear in 2(c). The two-dimensional Fourier transform of 2(c) is shown in 2(d). The points result from the atomic lattice, and the cigar-shaped peaks are due to the 1.3-nm corrugations. Diffuse peaks of this sort should be observable by x-ray diffraction, which could also be used to find the temperature dependence of the 1.3-nm corrugations. STM cannot be used for this purpose, since the surface degrades if the sample is ever warmed above 40–50 K [5,7].

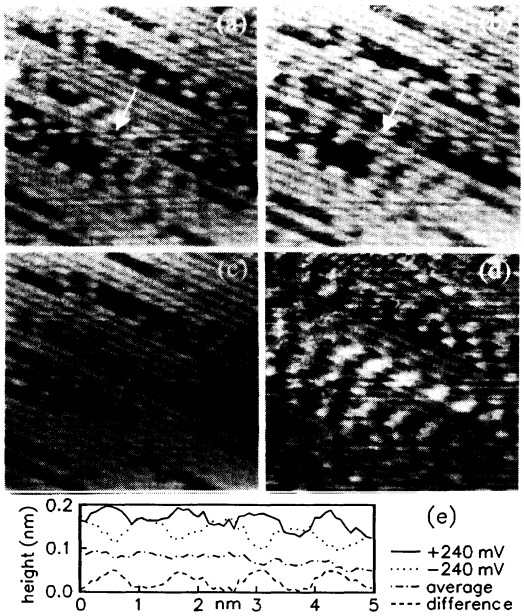

FIG. 1. Reversed-bias images, 10 nm on a side, of the CuO chain layer in 123. The images were obtained at sample bias values of (a) +240 mV and (b) −240 mV, showing empty and filled states, respectively. (c) The average of (a) and (b), and (d) is their difference. (e) A cross section along the CuO chain marked by the end points of the arrows in (a) and (b). The average tunneling current was 40 pA, and $T = 20$ K.

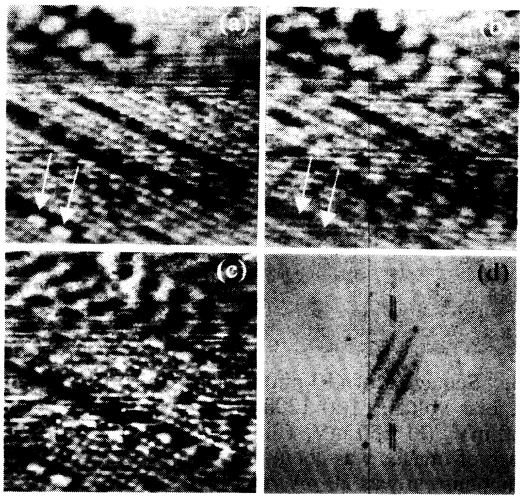

FIG. 2. Atomically resolved reversed-bias images, 10 nm on a side, of the CuO chain layer in 123. The images were obtained at sample bias of (a) +240 mV and (b) −240 mV, showing empty and filled states, respectively. (c) The difference of (a) and (b), and (d) is a Fourier transform of (c). The average tunneling current was 40 pA, and $T = 20$ K.

The atomic resolution in Fig. 2 shows another interesting feature. In the lower left-hand corner of 2(a), there are two bright bumps marked with arrows which do not appear in 2(b). Bumps that only appear under positive sample bias indicate the presence of atoms with mainly empty states near the Fermi level. Since oxygen often assumes a doubly negative charge in the bulk, it is likely that an isolated oxygen ion would have empty states near the Fermi level. This bias dependence of atomic bumps raises the question of whether the atomic bumps along continuous CuO chains may correspond to oxygen under positive bias and copper under reversed bias. At this time, we are unable to determine whether there was hysteresis in the reversed-bias imaging at the 0.1-nm level, so we cannot address this issue.

STM and STS studies of 123 [9] have often found asymmetric $I(V)$ curves. From our reversed-bias images, it is apparent that an asymmetry of this sort is possible due to the bias-dependent corrugations at the surface; if the tip is over a filled-state maximum, then the negative-bias side of the $I(V)$ curve would be enhanced. This highlights the need for good atomic-resolution STM to understand STS results. In addition, if the CuO chains are in a CDW state (as discussed below), there would be an energy gap [10] along the chains. Since STM tunneling does not occur solely in the direction normal to the sample surface, a **b**-direction gap could influence STS data taken on a **c**-axis-normal surface, obscuring features related to the CuO_2 planes.

Figure 3 shows a sequence of six images taken at several positive sample bias values. The detailed features in the 250 mV image was reproduced after the measurement, indicating that the STM imaging did not damage the sample. To ascertain that there was a vacuum gap

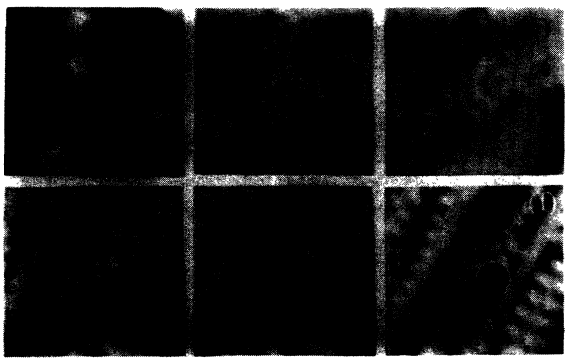

FIG. 3. Sequence of $(10\ \text{nm})^2$ images at a series of positive sample bias voltages [(a) 1200 mV, (b) 720 mV, (c) 480 mV, (d) 310 mV, (e) 250 mV, (f) 130 mV]. The drift over the sequence of images was about 3 nm (see circles). The average tunneling current was 20 pA, and $T = 20$ K.

between the tip and the sample for the different sample biases employed, the tunneling barrier height was measured between images. The value obtained was 0.8 ± 0.2 eV, in accord with that obtained for fresh samples in previous work [5].

The drift over the one-hour imaging sequence is 1/3 of the image width. Thus features can be traced throughout the sequence. For instance, the bright swell in the lower left corner of Fig. 3(a) changes into a dark swell in Fig. 3(b), and gradually evolves into a depression along a CuO chain in the lowest-bias images. In earlier work (Fig. 6 of Ref. [5]), we saw high-bias images similar to Fig. 3(a), and speculated that the "broad swells and depressions" might be due to oxygen ordering or vacancies. Here we see that these features are high-bias manifestations of the several-nm depressions along the chains, which are due to oxygen vacancies.

STM has been used successfully by several groups to detect CDW in low-dimensional systems [11]. Thus, the logical starting point in interpreting the corrugations along the one-dimensional CuO chains is to discuss the possibility that they represent a CDW state.

The standard theory of CDW transitions predicts several features of the electronic structure in the CDW state of a 1D metal [10]. First, the wave vector associated with the CDW modulation should be twice the Fermi wave vector, or $q_{\text{CDW}} = 2k_F$. Second, the CDW transition opens a gap at the Fermi level in the band, with both band extrema located at k_F. The empty electron states just above the CDW gap are spatially 180° out of phase with the filled electron states immediately below the CDW gap. Physically, this is due to the fact that the concentrations of positive ionic charge along the CDW attract the electrons, whereas the holes tend to lie where the ionic charge density is less positive; this is the driving force for the CDW.

Our data satisfy these two requirements. The positive- and negative-sample-bias images, which represent empty and filled states, respectively, support this picture, since the 1.3-nm corrugations along the CuO chains shift phase by 180° under bias polarity reversal. Now we estimate the Fermi wave vector in the CuO chains.

If we assume that the relevant CuO chain states are described by the one-dimensional CuO chain band in the well-known 123 Fermi surface [12] and note that most of the states have a Γ-Y axis projection which lies 25%–30% along the Γ-Y axis from the Γ (zone center) point, we estimate that the Fermi wave vector of the relevant chain states should be $2.0–2.5\ \text{nm}^{-1}$. This can be checked from charge-balance arguments, as follows. The hole density in the CuO_2 planes has been measured by the Hall effect [13] to be 0.2 hole per unit cell per CuO_2 plane. Assuming Y^{3+}, Ba^{2+}, Cu^{2+}, and O^{2-}, and adding 0.2 hole to each CuO_2 plane in the unit cell, leaves 0.6 hole, or a roughly 1/3-full band in the CuO chains. This is close to the 25%–30% filling value obtained from the Fermi surface shape. This value of the Fermi wave vector gives $q_{\text{CDW}} = 4.5\ \text{nm}^{-1}$, or a CDW-modulation wavelength of 1.3–1.6 nm, a range which is in accord with our experimental result of 1.3 ± 0.1 nm. Thus, our experimental data satisfy these two requirements for a CDW state. Our experimental value for the CDW wavelength of 1.3 ± 0.1 nm gives a Fermi wave vector of $2.4 \pm 0.2\ \text{nm}^{-1}$ in the CuO chain band.

CDW states can be static or dynamic [10]. In a homogeneous material, STM should be unable to detect the modulations of a dynamic CDW. However, in the presence of defects, a dynamic CDW can be locally pinned, resulting in modulations which are accentuated near the defect and decay away from it. This is what we observe in the CuO chain images, near a depression. The 1.3-nm corrugations are strongest near the depressions (oxygen vacancies) in the chain. The fact that an oxygen vacancy causes the STM image of the CuO chain to be depressed can be understood by considering the effect of oxygen removal on doping. An oxygen vacancy removes a hole locally [14]. This depresses the local conductivity, so that the STM tunneling current is lower over a chain with an oxygen vacancy nearby, and a depression is formed in the STM image.

The two above requirements are necessary, but they are not sufficient to fully determine that the CuO chains participate in a CDW state. The reversed-bias states being 180° out of phase can be argued for the case of a general symmetry-breaking transition, e.g., originally homogeneous electron states are redistributed into a set of states with alternating maxima, which add to a constant local density of states. Also, the wave vector of the electronic modulations should be twice the Fermi wave vector for any sort of real-space features due to electronic states near the Fermi surface. So, it is appropriate to consider other explanations of our data.

The simplest is that the modulations are caused by the electrons scattering off of the oxygen vacancies, or Friedel oscillations, similar to those seen in two-dimensional electron gases on noble metal (111) surfaces [15]. While this phenomenon could explain our results, it is not

adequate to explain the PDF data [1]. If a standing wave in the electron density did displace the ions, this should not have a sharp onset, as was observed by PDF, but rather would be gradually smeared out with increasing temperature. For this reason, we rule out electronic Friedel oscillations as an explanation for our data.

Egami interprets his PDF data in terms of a bipolaron mechanism of HTSC [1]. In this scenario, our results would be due to the scattering of CuO_2-plane bipolarons from the crystal field of oxygen vacancies. We are unable to distinguish between bipolaron scattering and CDW on the basis of the current data. In addition, lattice instabilities have been known to accompany HTSC due to strong electron-lattice interactions, without a causal relation between the two [16]. Nonetheless, either of these phenomena would have important implications for HTSC. If the electronic modulations are due to the scattering of CuO_2-plane bipolarons, this would point strongly toward the possibility that bipolarons form the superconducting state [17]. On the other hand, a CDW transition in the CuO chains would modify the interpretation of many experimental results obtained on 123 and 124, as follows.

The formation of a superconducting state is accompanied by a shift in the Fermi energy, of several meV in the case of HTSC [18]. This is because the superconducting transition lowers the electrons' free energy; a similar effect may occur for other collective phenomena, such as a CDW transition. Thus, in a system like 123 or 124 which has a metallic component (doped CuO_2 planes) that undergoes a superconducting transition and a 1D component (CuO chains) which is susceptible to a CDW transition, it is likely that each of these two collective phenomena will affect the energetics of the other. As the CuO_2 planes become superconducting, they may pull extra charge from the CuO chains, assisting the onset of the CDW transition, or the converse. This would be consistent with the fact that PDF data shows that the onset of correlated ionic motion is near or above the superconducting T_c.

An important implication of this type of interaction between collective phenomena in the CuO chains and the CuO_2 planes is that, since each separately has a characteristic temperature dependence, their interaction should alter the temperature dependence of the combined system. Thus superconducting properties such as the magnetic penetration depth may exhibit an anomalous temperature dependence because the CuO chains modify the energetics of charge transfer. Similarly, spectroscopic measurements such as photoemission or scanning tunneling spectroscopy, when interpreted in terms of superconductivity alone, may seem exotic, when they really just need to be disentangled from the effects of a CDW state in the CuO chains. In this context, it is important to take care in drawing conclusions from spectroscopic and temperature-dependent experimental data on 123 and 124.

In conclusion, we have used reversed-bias STM to explore the CuO chain layer of 123. We find 1.3-nm corrugations that change sign under bias polarity reversal, and that some atomic bumps appear only under positive sample bias. The former result is consistent with a CDW in the CuO chains, the latter with bias-selective imaging of oxygen ions. In addition, we have taken images at a series of biases, finding that broad swells and depressions are high-bias manifestations of the several-nm depressions in the CuO chains, which we attribute to oxygen vacancies.

We acknowledge conversations with D. Tanner, Q. Niu, A. Sleight, M. Flatte, and J. Goodenough. This work is supported by Texas ARP No. 172, ARP No. 403, and NSF DMR-9158089.

*To whom correspondence should be addressed.

[1] T. Egami *et al.*, in Proceedings of the OE/LASE '94 Conference, SPIE, Los Angeles, 1994 (to be published).
[2] S. D. Conradson, I. D. Raistrick, and A. R. Bishop, Science **248**, 1394 (1990); R. P. Sharma *et al.*, Physica (Amsterdam) **174C**, 409 (1991).
[3] L. D. Rotter *et al.*, Phys. Rev. Lett. **67**, 2741 (1991).
[4] R. Fehrenbacher, Phys. Rev. B **49**, 12 230 (1994).
[5] H. L. Edwards, J. T. Markert, and A. L. de Lozanne, Phys. Rev. Lett. **69**, 2617 (1992).
[6] H. L. Edwards, J. T. Markert, and A. L. de Lozanne, J. Vac. Sci. Tech. B **12**, 1886 (1994).
[7] M. Lindroos *et al.*, Physica (Amsterdam) **212C**, 347 (1993).
[8] N. Schroeder *et al.*, Physica (Amsterdam) **217C**, 220 (1993).
[9] T. Hasegawa, H. Ikuta, and K. Kitazawa, in *Physical Properties of High Temperature Superconductors III*, edited by D. M. Ginsburg (World Scientific, Singapore, 1992).
[10] A. W. Overhauser, Adv. Phys. **27**, 843 (1978).
[11] Z. Dai, C. G. Slough, and R. V. Coleman, Phys. Rev. Lett. **66**, 1318 (1991).
[12] W. E. Pickett *et al.*, Science **255**, 46 (1992).
[13] Z. Z. Wang *et al.*, Phys. Rev. B **36**, 7222 (1987).
[14] N. Chandrasekhar, O. T. Valls, and A. M. Goldman, Phys. Rev. Lett. **71**, 1079 (1993).
[15] Y. Hasegawa and P. Avouris, Phys. Rev. Lett. **71**, 1071 (1992); M. F. Crommie, C. P. Lutz, and D. M. Eigler, Nature (London) **363**, 524 (1993).
[16] W. E. Pickett, Rev. Mod. Phys. **61**, 433 (1989).
[17] J. B. Goodenough, J.-S. Zhou, and J. Chan, Phys. Rev. B **47**, 5275 (1993); D. Emin, Phys. Rev. Lett. **72**, 1052 (1994).
[18] D. van der Marel and G. Rietveld, Phys. Rev. Lett. **69**, 2575 (1992); D. I. Khomskii and F. V. Kusmartsev, Phys. Rev. B **46**, 14 245 (1992).

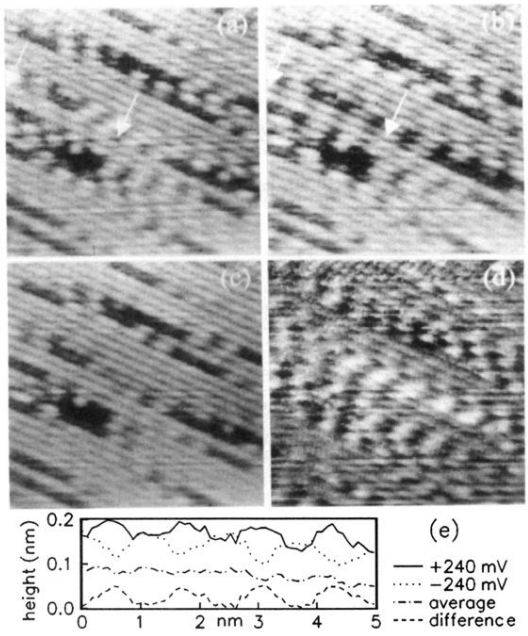

FIG. 1. Reversed-bias images, 10 nm on a side, of the CuO chain layer in 123. The images were obtained at sample bias values of (a) +240 mV and (b) −240 mV, showing empty and filled states, respectively. (c) The average of (a) and (b), and (d) is their difference. (e) A cross section along the CuO chain marked by the end points of the arrows in (a) and (b). The average tunneling current was 40 pA, and $T = 20$ K.

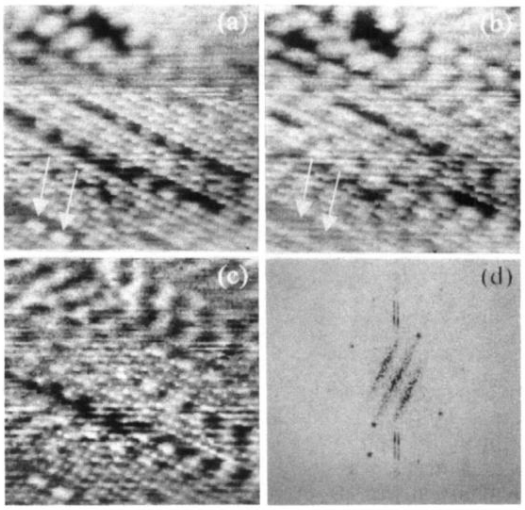

FIG. 2. Atomically resolved reversed-bias images, 10 nm on a side, of the CuO chain layer in 123. The images were obtained at sample bias of (a) +240 mV and (b) −240 mV, showing empty and filled states, respectively. (c) The difference of (a) and (b), and (d) is a Fourier transform of (c). The average tunneling current was 40 pA, and $T = 20$ K.

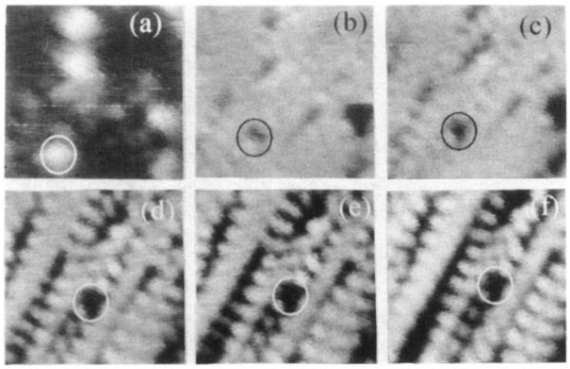

FIG. 3. Sequence of $(10\ \text{nm})^2$ images at a series of positive sample bias voltages [(a) 1200 mV, (b) 720 mV, (c) 480 mV, (d) 310 mV, (e) 250 mV, (f) 130 mV]. The drift over the sequence of images was about 3 nm (see circles). The average tunneling current was 20 pA, and $T = 20$ K.